Neurobiology of Aging 113 (2022) 108–117

Contents lists available at ScienceDirect

Neurobiology of Aging

journal homepage: www.elsevier.com/locate/neuaging.org

Oligomeric α-Synuclein induces skin degeneration in reconstructed human epidermis

Júlia T. Oliveira[a], Vanja Dakic[b], Gabriela Vitória[a], Carolina da S.G. Pedrosa[a], Mayara Mendes[a], Luiz Guilherme H.S. Aragão[a], Thyago R. Cardim-Pires[d], Damien Lelièvre[e], Daniel Rodrigues Furtado[a], Roberta O. Pinheiro[f], Débora Foguel[d], Lionel Breton[g], Charbel Bouez[h], Rodrigo De Vecchi[b], Marília Zaluar P. Guimarães[a,c,#], Stevens Rehen[a,i,#,*]

[a] D'Or Institute for Research and Education (IDOR), Rio de Janeiro, RJ, Brazil
[b] L'Oréal Research & Innovation, Rio de Janeiro, Brazil
[c] Instituto de Ciências Biomédicas, Universidade Federal do Rio de Janeiro (UFRJ), Rio de Janeiro, RJ, Brazil
[d] Instituto de Bioquímica Médica, Universidade Federal do Rio de Janeiro (UFRJ), Rio de Janeiro, RJ, Brazil
[e] EPISKIN SA, Lyon, France
[f] Leprosy Laboratory, Oswaldo Cruz Institute (IOC), Oswaldo Cruz Foundation (Fiocruz), Rio de Janeiro, RJ, Brazil
[g] L'Oréal Research & Innovation, Aulnay-sous-bois, France
[h] L'Oréal Research & Innovation, Clark, NJ, USA
[i] Departamento de Genética, Instituto de Biologia, Universidade Federal do Rio de Janeiro (UFRJ), Rio de Janeiro, RJ, Brazil

ARTICLE INFO

Article history:
Received 21 September 2021
Revised 18 February 2022
Accepted 19 February 2022
Available online 26 February 2022

Keywords:
Epidermis
Skin degeneration
Inflammaging
Neurodegeneration
α-Synuclein

ABSTRACT

Aged and photoaged skin exhibit fine wrinkles that are signs of epidermal inflammation and degeneration. It has been shown that healthy elderly skin expresses amyloidogenic proteins, including α-Synuclein, which are known to oligomerize and trigger inflammation and neurodegeneration. However, little is known about their putative role in skin physiology and sensitivity. To unravel this possible role, we investigated the impact of oligomeric α-Synuclein (Oα-Syn) in 2D and 3D keratinocyte human models. Exogenous Oα-Syn caused degeneration of reconstructed human epidermis (RHE) by diminishing proliferation and thickness of the stratum basale. Oα-Syn also increased NF-kB nuclear translocation in keratinocytes and triggered inflammation in the RHE, by increasing expression of interleukin-1β and tumor necrosis factor-alpha, and the release of tumor necrosis factor-alpha in a time-dependent manner. Dexamethasone and an IL-1β inhibitor partially diminished RHE degeneration caused by Oα-Syn. These findings suggest that Oα-Syn induces epidermal inflammation and decreases keratinocyte proliferation, and therefore might contribute to epidermal degeneration observed in human skin aging.

1. Introduction

The epidermis is the outermost layer of the skin and is mainly composed of keratinocytes. The proliferation of keratinocytes is restricted to the basal layer, which is crucial to skin homeostasis and regeneration. Chronological skin aging, which is accompanied by epidermal degeneration, is a natural process that occurs throughout life. However, it can be accelerated by some factors, such as smoking (Martires et al., 2009) and ultraviolet (UV) exposure (Baumann, 2007). Aged skin displays high levels of inflammatory mediators including the proinflammatory cytokine tumor necrosis factor-alpha (TNF-α). Many pro-inflammatory agents, including TNF-α, trigger the RelA/p65 NF-kB subunit translocation to the nucleus, thereby regulating various processes including cell proliferation and further expression of itself and other inflammatory cytokines (Joyce et al., 2001; Lan et al., 2005; Pupe et al., 2003). NF-κB plays a pivotal role in skin homeostasis and aging (Grinberg-Bleyer et al., 2015).

Abbreviations: α-Syn, α-Synuclein; Oα-Syn, oligomeric α-Synuclein; IL, interleukin; TNF-α, tumor necrosis factor-alpha; UV, ultraviolet; NF-κB, nuclear factor kappa-light-chain-enhancer of activated B cells; Aβ, β-Amyloid; RHE, reconstructed human epidermis; HEKn, human neonatal epidermal keratinocytes; PBS, phosphate-buffered saline; DMEM, Dulbecco's Modified Eagle Medium; DAPI, 4′,6-diamidino-2-phenylindole.

* Corresponding author: Federal University of Rio de Janeiro (UFRJ) and D'Or Institute for Research and Education (IDOR). Tel: +55 21 3883 6000.
E-mail address: srehen@lance-ufrj.org (S. Rehen).
# These authors contributed equally to this work.

0197-4580/$ – see front matter © 2022 The Authors. Published by Elsevier Inc. This is an open access article under the CC BY license (http://creativecommons.org/licenses/by/4.0/)
https://doi.org/10.1016/j.neurobiolaging.2022.02.010

Aggregation of amyloidogenic proteins in the central nervous system, such as α-Synuclein (α-Syn) and β-Amyloid (Aβ), are the pathological hallmarks of neurodegenerative processes underlying Parkinson's and Alzheimer's diseases, respectively. The leading molecular signature in Parkinson's disease is the accumulation of misfolded α-Syn, including oligomeric α-Syn (Oα-Syn), in dopaminergic neurons of the substantia nigra. Oligomers with different morphologies and fibrils of α-Syn are toxic species of this protein, which can be influenced by post-transcriptional modifications, including phosphorylation, and aggregates. Both species are involved in the pathophysiology of neurodegeneration (Lashuel et al., 2013).

A growing body of evidence demonstrates abnormal aggregates in other tissues with consequences to physiology and pathology (Beach et al., 2010; Braak and Del Tredici, 2017; Gelpi et al., 2014; Wakabayashi et al., 1990). For instance, neurodegenerative disease-related proteins, such as tau, Aβ34, and α-Syn, were found in the epidermal layer of human skin (Akerman et al., 2019; Rodriguez-Leyva et al., 2017). In the case of Parkinson's disease, α-Syn substantially accumulates in the epidermis of patients but also occurs in healthy individuals to a lesser extent (Rodriguez-Leyva et al., 2017). Although studies have detected α-Syn and other amyloidogenic proteins in human skin, how they affect skin homeostasis is not clear yet. Evidence from studies in the nervous system suggests inflammation among the consequences of protein misfolding (Alvarez-Erviti et al., 2011).

In this work, we aimed to investigate the possible functional role(s) of exogenous Oα-Syn in 2D and 3D keratinocyte models, the last termed reconstructed human epidermis (RHE).

2. Materials and methods

2.1. Cell culture

2.1.1. Human Epidermal Keratinocytes, neonatal (HEKn)

Human neonatal epidermal keratinocytes (HEKn) (Life Technologies - C0015C) were cultivated in EpiLife Medium (Thermo Fisher Scientific - MEPI500CA) with 1x HKGS (Thermo Fisher Scientific - S-001-5) on a T75 culture flask. When HEKn achieved 80% of confluence, they were split with TrypLE Express Enzyme (1X) (Thermo Fisher Scientific - 12605028) for 10 minutes, counted, and centrifuged at 200 x *g* for 10 minutes. Then, the cells were replated at 3×10^5 cells per T75 culture flask or at 1.2×10^4 cells per well in 96-well plates and maintained in an incubator at 37 °C with 5% CO2. The medium was changed every other day. For the inflammatory inhibition assay, HEKn were pretreated for 2 hours with dexamethasone (Diprospan, 10 μM) or IL-1β inhibitor (Kineret, 25 μg/mL), which were added or not at the time Oα-Syn was administered. The TNF-α inhibitor (Etanercept, 500 μg/mL) was administered at the same time as Oα-Syn, and the incubation carried on for 24 hours.

2.1.2. Reconstructed Human Epidermis (RHE)

SkinEthic RHE was reconstructed *in vitro* from healthy human keratinocytes, which were donated by volunteers with signed consent terms, and expanded before use. RHE was grown on an inert polycarbonate filter (0.5 cm^2) at the air-liquid interface, in a chemically defined medium (Rosdy and Clauss, 1990). The RHE is a multilayered human epidermis model, with clearly visible basal, spinous, granular, and corneal layers. This model features a functional permeability barrier and is reliable to test skin permeability and toxicity (Tornier et al., 2010). Each RHE batch was checked according to standard quality control criteria, and the tests included viability, barrier function, and morphology (Vecchi et al., 2018). Seventeen-day-old RHEs were used in the experiments as this is the time point when maturity is achieved, meaning they have all layers completely formed. All substances tested were administered from the stratum basale side.

2.2. Oligomer preparation and characterization

2.2.1. α-Synuclein (α-Syn)

Wild-type α-Syn monomers were expressed and purified according to Krüger et al. (1998). A step was added to the purification procedure to remove lipopolysaccharide, a bacterial endotoxin, that could interfere with the results in cell culture assays. To obtain a lipopolysaccharide-free protein, purified α-Syn monomers were passed through a polymyxin B-conjugated resin (Detoxi-gel endotoxin removing column, Thermo Scientific, Waltham, MA, USA). Oα-Syn was produced by incubating 120 μM monomers in PBS for 18 hours at pH 7.5, 37°C under stirring (800 RPM) in a thermomixer. The presence of oligomers was confirmed by transmission electron microscopy imaging and dot blot assay (Supplementary Fig. 1). The definition of oligomer used in the present work is of a heterogeneous population, with non-fibrillary structure, sometimes amorphous or with a ring-like appearance, which size can be probed by transmission electron microscopy (Braga et al., 2011; Fernandes et al., 2020; Kumar et al., 2020; Montoliu-Gaya et al., 2017).

2.2.2. Transmission electron microscopy

Copper grids (carbon- and formvar-coated 400 mesh) (Electron Microscopy Sciences, Hatfield PA) were glow discharged and 5 μL of the sample was applied for 5 minutes. The excess sample was removed with filter paper and the grids were immediately incubated with 2% uranyl acetate solution for 5 min. The excess stain was removed and the grid was allowed to dry thoroughly. Grids were then examined on a Tecnai Spirit (FEI Company) microscope at 120 kV.

2.2.3. Dot-blot

Samples were blotted on nitrocellulose membranes (0.45 μm, Bio-Rad) and incubated for 1 hour with 10% skimmed milk. Membranes were washed using Tris-buffered saline with 0.05% Tween 20, incubated with A11 antibody (1:1000, anti-oligomers; AHB0052, ThermoFisher), OC antibody (1:1000; anti-amyloid fibrils; AB2286, Sigma-Aldrich), and anti-α-synuclein (1:1000; AHB0261, ThermoFisher) for 2 hours at 25°C, and, then, incubated with horseradish peroxidase-conjugated secondary antibody (1:2000; Sigma). Membranes were revealed using an ECL Plus kit (GE Healthcare).

2.3. Sample preparation and immunostaining

RHEs and HEKn were fixed in 4% paraformaldehyde for 20 minutes and washed 3 times in PBS. RHE samples were embedded in a Tissue-Tek OCT compound and frozen in liquid nitrogen. Longitudinal cryosections were cut at 10 μm on a cryostat (Leica CM 1850) and mounted on gelatin precoated slides. The immunostaining procedure occurred as follows. Samples were permeabilized with 0.3% triton x-100 for 15 minutes, blocked in 3% bovine serum albumin for 1 hour at room temperature, and incubated overnight at 4°C in 2% blocking solution containing diluted primary antibodies. Then, samples were washed 3 times in PBS, reblocked for 20 minutes, and incubated with corresponding secondary antibodies diluted in 2% blocking solution for 40 minutes at room temperature. Finally, samples were rinsed 3 times in PBS, stained with the nuclear marker 4′,6-diamidino-2-phenylindole (DAPI, 0.5 μg/mL) for 5 minutes, rinsed again 3 times in PBS, and slides were mounted

with Aqua-Poly-mount (Polysciences) or cell plate wells were covered with glycerol (Sigma). We used the following primary antibodies: mouse anti-Ki67 (1:50, 550609, BD Pharmigen); mouse anti-α-synuclein (1:200, AHB0261, Thermo Fisher Scientific); and mouse anti-NF-κB p65 (1:200, SC-8008, Santa Cruz Biotechnology). The secondary antibodies used were: Goat anti-Mouse IgG (H+L) Secondary Antibody, Alexa Fluor 488 conjugate (A-11001, Invitrogen); and Goat anti-Mouse IgG (H+L) Secondary Antibody, Alexa Fluor 594 conjugate (A-11032, Invitrogen).

The hematoxylin-eosin-safran staining was performed on paraffin sections using the Sakura Tissue-Tek Prisma automated slide stainer, according to the manufacturer's protocol.

2.4. Image acquisition

Images of immunostained RHE sections were acquired with a confocal microscope Leica TCS SP8 using a 63x objective lens, while images of immunostained HEKn were acquired with the high content screening microscope Operetta (PerkinElmer, Waltham, MA, USA) using a 40x objective lens. For capturing HEKn images, 9 fields per well were systematically selected.

2.5. Proliferation and nuclei quantification assays

HEKn and RHEs were immunostained for the proliferation marker Ki67 as described above. For RHE analysis, we quantified the percentage of total Ki67+ nuclei/ total DAPI+ nuclei using the ImageJ software. HEKn analysis, in turn, was performed with the software Columbus Image Data Storage and Analysis System (PerkinElmer), as follows. First, the total amount of nuclei was selected using the DAPI channel. Then, we found the Ki67+ nuclei using the Alexa 488 channel, which was the emission spectrum of the secondary antibody used, inside the pre-selected DAPI+ regions. Results were defined by the ratio of Ki67+ nuclei/ DAPI+ nuclei and plotted as the percentage of positive cells. Quantification of DAPI-stained HEKn nuclei was also used as an indicator of cell survival, and the results were presented as the percentage of DAPI+ nuclei relative to control.

2.6. NF-κB nuclear translocation assay

NF-kB nuclear translocation assay is based on the amount of nuclear NF-kB relative to its cytoplasmic counterpart. To establish the assay, HEKn and RHEs were treated with 2, 10, or 20 ng/mL TNF-α (TNA-H4211, ACROBIosystems, DE, USA) for 45 minutes, fixed with 4% paraformaldehyde for 30 minutes, and immunostained for the p65 (RelA) subunit of NF-κB. For the RHE analysis, we created a mask to identify the cytoplasms immunostained for NF-κB and the nuclei stained with DAPI using the same grayscale and threshold for all images. Immunostaining intensity from the two masks, which was represented as arbitrary units, was quantified and plotted as the ratio of nucleus/cytoplasm NF-κB fluorescence intensity. All RHE images (10 per sample) were processed and quantified using ImageJ software. Conversely, for HEKn analysis, we systematically selected 9 fields per image and used the high-content image analysis software Harmony 5.1 (PerkinElmer, Waltham, MA, USA) to generate the ratio of nucleus/cytoplasm intensity.

2.7. Quantitative RT-PCR (RT-qPCR)

RHE samples were sliced into thick sections, transferred to 2.0 mL pre-filled tubes with 1.5 mm Triple-Pure Zirconium homogenizer beads (Benchmark Scientific, USA), containing a fresh amount of Lysis Buffer (ThermoFisher Scientific, USA) plus 2-mercaptoethanol (1% v/v) (Sigma-Aldrich, USA) for each purification procedure, and shaken vigorously using the BeadBug Microtube Homogenizer apparatus (D1030-E, Benchmark Scientific). Subsequently, total RNA was isolated using the PureLink RNA Mini kit (ThermoFisher Scientific, USA) in accordance with the manufacturer's instructions. After isolation, RNA was treated with DNase I (ThermoFisher Scientific). RNA concentration and quality were quantified on a NanoDrop 2000c spectrophotometer (ThermoFisher Scientific) and integrity was evaluated by 2% agarose gel electrophoresis using a UV light photodocumentation system (L-PIX, Loccus Biotecnologia). One microgram of total RNA obtained from each sample was reverse transcribed into complementary DNA using SuperScript VILO Master Mix, according to the manufacturer's instructions (ThermoFisher Scientific). RT-qPCR reactions carried out with a total reaction volume of 10 µL containing 1X of each TaqMan designed primers [human; TNF (Hs99999043_m1), interleukin (IL)-1 (Hs01555410_m1), IL-6 (Hs00985639_m1), and IL-18 (Hs010003716_m1) ThermoFisher Scientific], TaqMan Universal Master Mix II, with UNG (ThermoFisher Scientific), and 10 ng of cDNA resuspended in UltraPure DNase/RNase-free distilled water. No reverse transcriptase control and no template controls were inserted into each assay. The reactions were amplified in a StepOnePlus Real-Time PCR Systems thermocycler (ThermoFisher Scientific) under standard conditions. Thermal cycling conditions comprised an initial incubation at 50°C for 2 minutes, 95°C for 10 minutes, 40 cycles of denaturation at 95°C for 15 seconds, and annealing and extension at 60°C for 1 minute. The relative expression of target genes was normalized by Glyceraldehyde-3-phosphate dehydrogenase (GAPDH; Hs99999905_m1). RT-qPCR data analysis was realized with the N_0 method implemented in LinRegPCR v. 2020.2. The results were obtained from 3 independent experiments containing 4 technical replicates, and, for the assay, duplicates for each sample were performed. For the analysis, the mean of data from each experiment was obtained and normalized by the mean of the housekeeping (GAPDH) from each experiment.

2.8. ELISA for TNF-α

To quantify the levels of TNF- α release in the RHE supernatant, the RHEs were challenged for 2 or 24 hours with 10 μM Oα-Syn. Each sample was a pool of the supernatants of at least 3 technical replicates from 3 independent experiments, and for the assay, we performed duplicates for each sample, which were kept frozen at -80°C until needed. Immediately after thawing, the samples were centrifuged at 600 x *g* for 5 minutes to remove particulates. Then, the samples were analyzed using the Human TNF-alpha quantikine ELISA kit (DTA00D, R&D systems) in accordance with the manufacturer's instructions. Absorbance at 450 nm with wavelength correction set to 540 nm was measured with a Tecan Infinite 200 PRO (Life Sciences, Switzerland) spectrophotometer.

2.9. Statistical analyses

Data were analyzed either by student t-test, one-way ANOVA or two-way ANOVA, followed by the Dunnett test, as applicable. A 95% confidence interval was accepted as statistically significant. All analyses were performed with GraphPad Prism software 8.0.

3. Results

3.1. Oα-Syn decreases RHE proliferation and thickness

α-Syn, particularly in melanocytes and sensory neurons (Rodriguez-Leyva et al., 2017), as well as Aβ (Heinonen et al., 1994), are found in samples from human skin biopsies. First, we

checked whether the RHEs also express α-Syn by immunostaining. We found α-Syn immunoreactivity in a few cells from the stratum basale of the RHEs (Supplementary Fig. 2).

Second, we investigated the possible toxic role of α-Syn in RHE biology. We challenged RHEs with exogenous 10 µM Oα-Syn or 20 ng/mL TNF-α for 24 hours. We noticed that some treated RHEs were apparently thinner than control ones. One hypothesis to explain this thinning could be an impairment in cell proliferation. We measured the thickness of the proliferative stratum of the RHEs and found that some treatments indeed reduced this dimension of the samples. Oα-Syn-challenged RHEs had a statistically significant thinner proliferative stratum (55.02 ± 3.53 µm) compared with control RHEs (67.5 ± 2.58 µm, $p < 0.01$). TNF-α-treated RHEs were also thinner, but the difference was not statistically significant (58.61 ± 0.66 µm) (Fig. 1A). Additionally, the RHE sections were immunostained for the proliferation marker Ki67 and quantified over total nuclei. Indeed, we found that TNF-α-challenged RHEs (2.18 ± 0.54%, $p < 0.05$) and, more pronouncedly, Oα-Syn-challenged RHEs (0.72 ± 0.3%, $p < 0.0001$) presented a lower percentage of Ki67 positive nuclei compared with controls (5.95 ± 0.71%) (Fig. 1B–E).

To further pursue the anti-proliferative effect of Oα-Syn, we questioned whether this action required a 3D tissue arrangement or if it would be present in isolated keratinocytes. HEKn were challenged for 24 hours with 10 µM Oα-Syn, fixed, and immunostained for Ki67. As expected, we observed that the percentage of Ki67 positive cells was lower in Oα-Syn-challenged HEKn at both 10 μM (56.5 ± 25.66%, $p < 0.0001$) and 30 μM (44.81 ± 37.01%, $p < 0.0001$) concentrations (Fig. 2). In addition, to certify that the aggregated α-Syn species, which is known as toxic, accounted for the decrease in keratinocyte proliferation, we compared the effects of monomeric and oligomeric α-Syn forms on the HEKn. The percentage of proliferative HEKn treated with monomeric α-Syn (96.32 ± 7.4) was comparable with controls (Fig. 2).

The reduction in the number of proliferative keratinocytes was quantified here as relative to the total cell amount because there was still the possibility that Oα-Syn may also cause cell death 24 hours following the insult. To rule this possibility in or out, we counted the total number of nuclei from HEKn that had been treated with 10 μM Oα-Syn and controls. We found that the number of nuclei from Oα-Syn-challenged HEKn (91.5 ± 4.86%) was comparable with controls (100 ± 4.2%), suggesting that no significant cell death took place under these conditions (Supplementary Fig. 3).

3.2. Oα-Syn prompts NF-kB nuclear translocation in keratinocytes

NF-kB nuclear translocation is considered key for the aging process, and several senescence pathways converge through NF-kB (Wang et al., 2019). Together with the fact that Oα-Syn causes inflammation in the nervous system, we asked if it could have decreased keratinocyte proliferation by eliciting an inflammatory response such as activation of the NF-kB pathway.

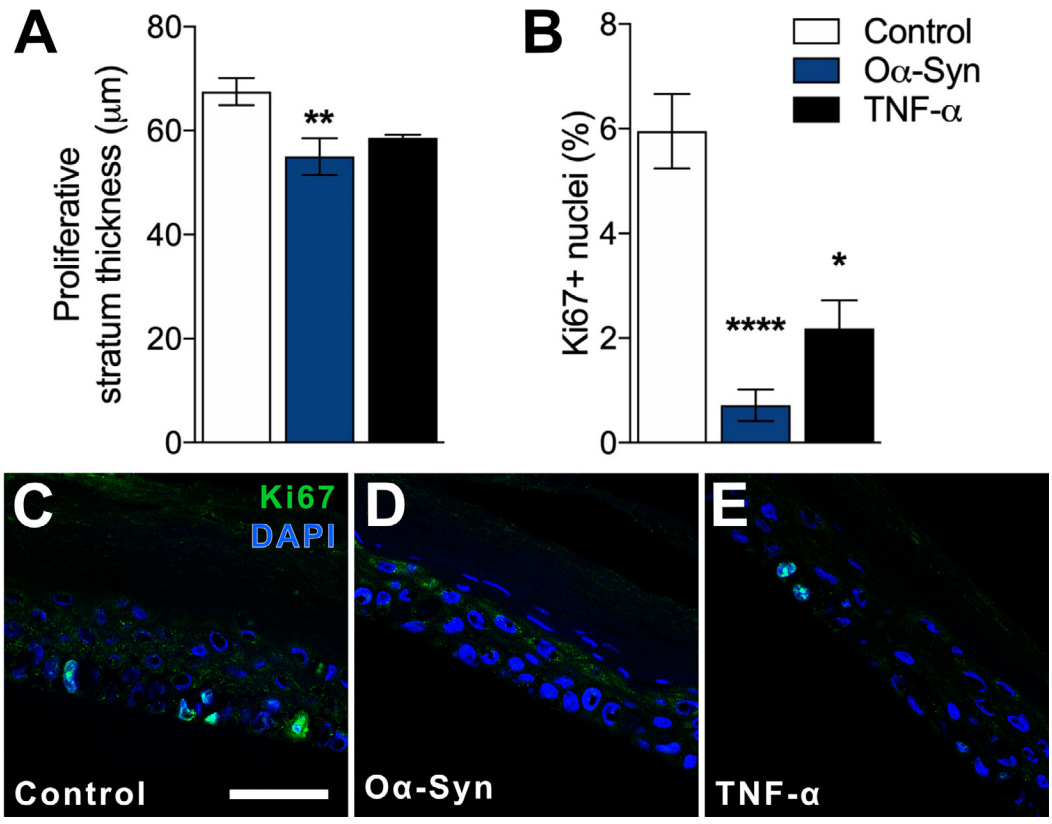

Fig. 1. Oligomeric α-Synuclein (Oα-Syn) and tumor necrosis factor-alpha (TNF-α) decreased keratinocyte proliferation in RHE. (A) Measurement of the thickness of the RHE proliferative stratum (n = 3 experiments, plotted as average ± SEM, analyzed by one-way ANOVA followed by Dunnett' post-hoc test; $^{**}p < 0.01$). (B) Percentage of Ki67 + nuclei relative to total nuclei (n = 3 experiments, plotted as average ± SEM, analyzed by one-way ANOVA followed by Dunnett' post-hoc test; $^{*}p < 0.05$, $^{****}p < 0.0001$) (C, D, E) Photomicrographs of control and challenged RHE with 10 μM Oα-Syn or 20 ng/mL TNF-α for 24 hours, and immunostained for Ki67 (green) and counterstained with DAPI (blue). Scale bar: 50 μm. Abbreviations: DAPI, 4′,6-diamidino-2-phenylindole; RHE, reconstructed human epidermis. (For interpretation of the references to color in this figure legend, the reader is referred to the Web version of this article.)

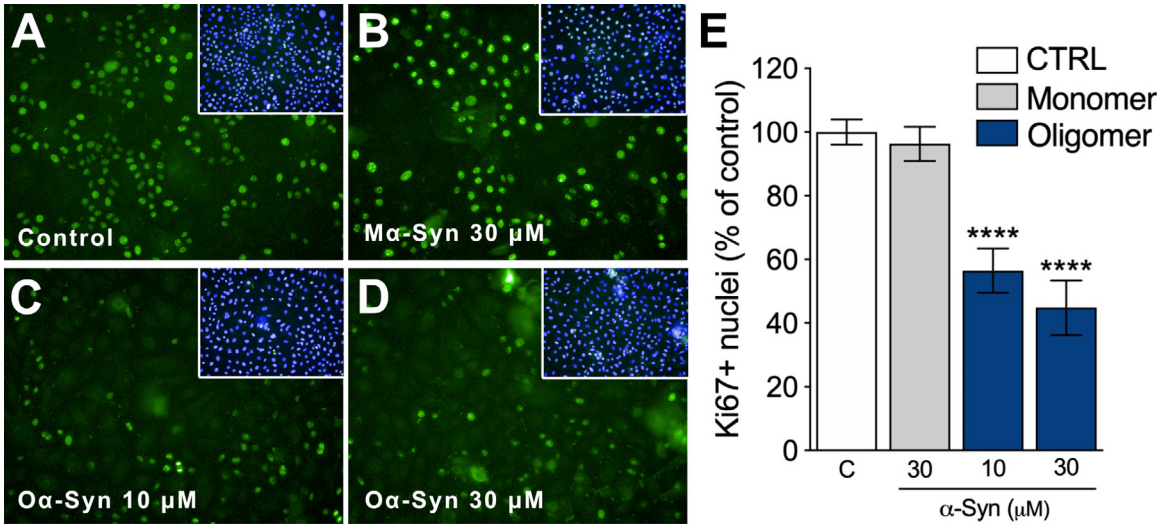

Fig. 2. Oligomeric (Oα-Syn) but not monomeric α-Synuclein (Mα-Syn) causes a decrease in HEKn proliferation. (A–D) Photomicrographs of control and HEKn challenged with Oα-Syn (10 μM or 30 μM) or Mα-Syn (30 μM) for 24 hours, immunostained for Ki67 (green) and counterstained with DAPI (blue, insets). (E) Percentage of Ki67 + cells relative to control (CTRL) (n = 3 experiments, plotted as average ± SEM, analyzed by one-way ANOVA followed by Dunnett' post-hoc test; $^{****}p < 0.0001$). Scale bar: 50 μm. Abbreviations: DAPI, 4′,6-diamidino-2-phenylindole; HEKn, human neonatal epidermal keratinocytes. (For interpretation of the references to color in this figure legend, the reader is referred to the Web version of this article.)

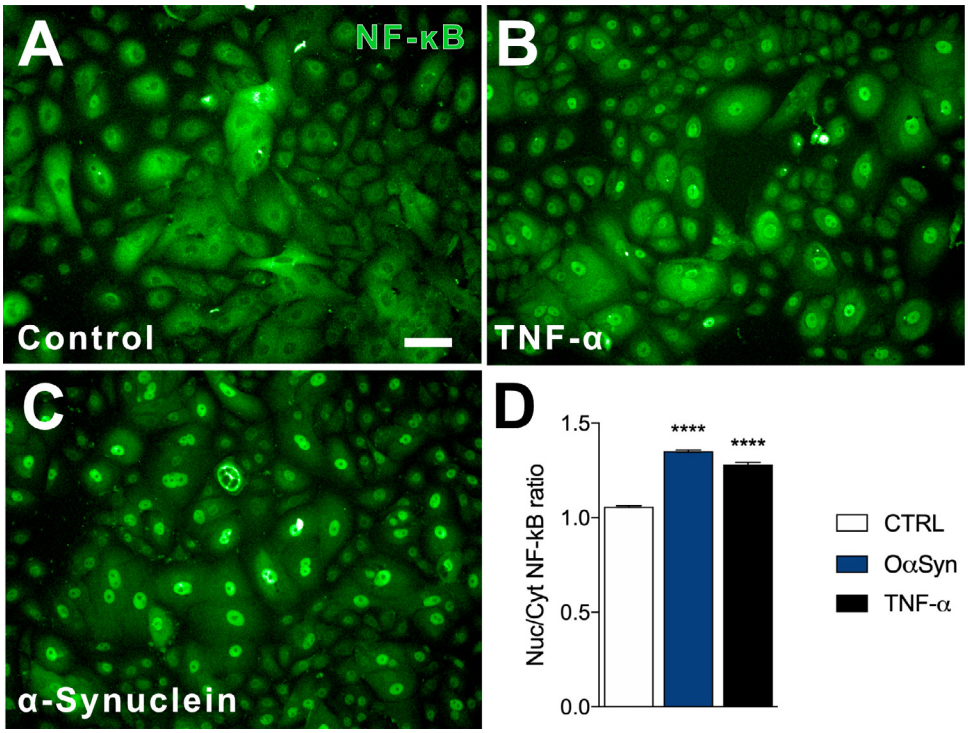

Fig. 3. Oligomeric α-Synuclein (Oα-Syn) 45 minutes-treatment triggers nuclear factor-κB (NF-kB) translocation to the nucleus in HEKn. (A–C) Photomicrographs of control (CTRL), Tumor necrosis factor-alpha (TNF-α)- and Oα-Syn-challenged HEKn immunostained for NF-kB. (D) Nucleus/cytoplasm NF-kB fluorescence intensity ratio (n = 2 experiments, plotted as average ± SEM, analyzed by one-way ANOVA followed by Dunnett' post-hoc test; $^{****}p < 0.0001$). Scale bar: 50 μm. Abbreviation: HEKn, human neonatal epidermal keratinocytes.

First, we established the NF-kB nuclear translocation response in HEKn and RHE. For this, we challenged HEKn with 2, 10, and 20 ng/mL TNF-α for 45 minutes and observed that TNF-α increased the nuclear/cytoplasm ratio of NF-kB fluorescence intensity at all tested concentrations (1.69 ± 0.03, $p < 0.001$; 1.64 ± 0.04, $p < 0.05$; and 1.68 ± 0.02, $p < 0.001$, respectively) compared with control (1.29 ± 0.07) (Supplementary Fig. 4). Because the RHE is a tridimensional structure composed of layers, we challenged it for 45 minutes only with the highest concentration that induced the translocation response in HEKn, which was 20 ng/mL, applied from the stratum basale side. We found that this insult also increased the nucleus/cytoplasm NF-kB fluorescence intensity in RHEs compared with controls (0.94 ± 0.02 and 0.63 ± 0.03, respectively, $p < 0.001$) (Supplementary Fig. 4). These results confirmed that keratinocytes in 2D and 3D cultures efficiently exhibit the NF-kB nuclear translocation response following insult with TNF-α.

Next, we challenged HEKn with 10 μM Oα-Syn or 20 ng/mL TNF-α for 45 minutes and analyzed the NF-kB nuclear translo-

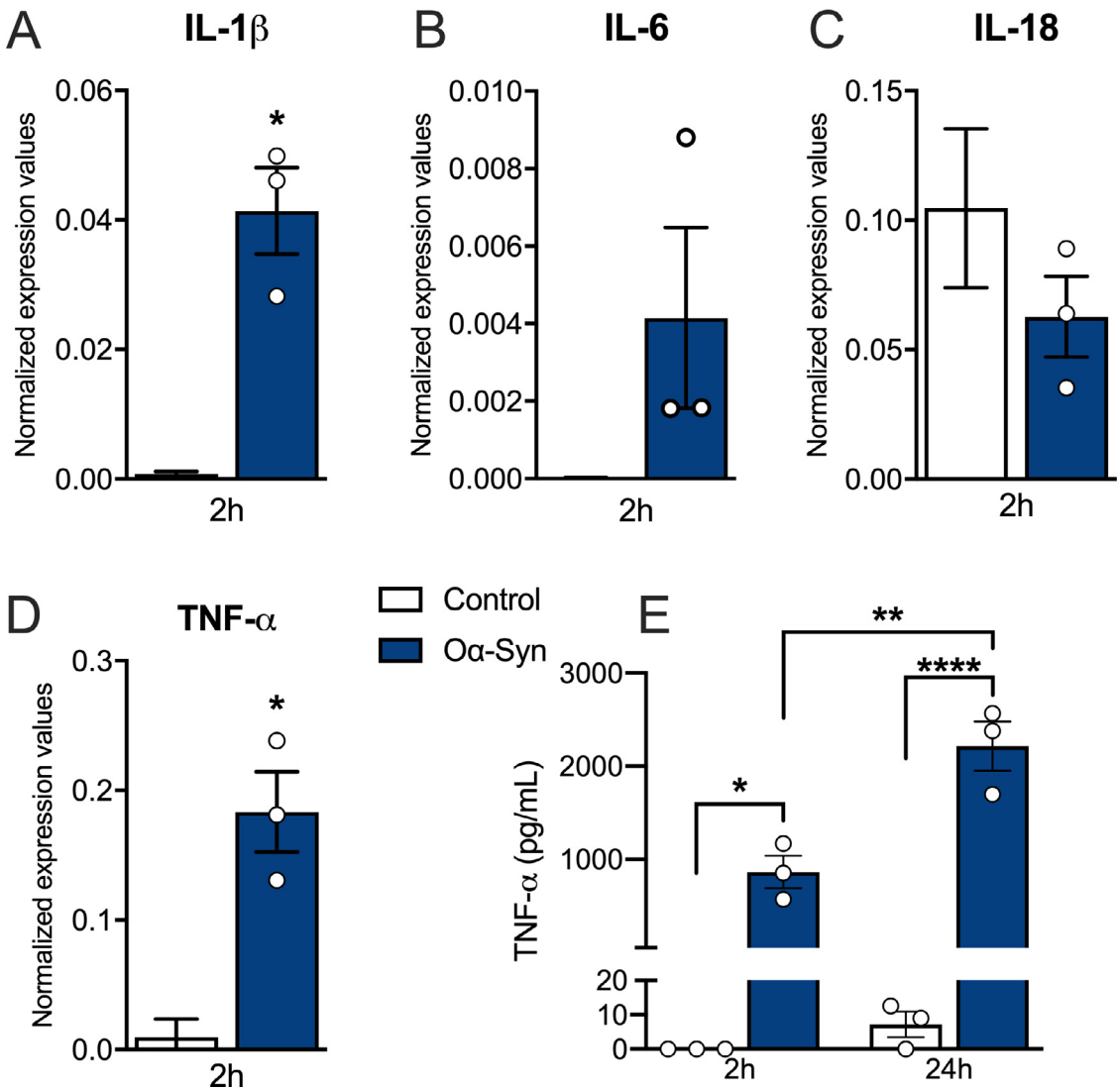

Fig. 4. Oligomeric α-Synuclein (Oα-Syn) induces tumor necrosis factor-alpha (TNF-α) and interleukin (IL)-1β expression and the release of TNF-α by the RHE. (A–D) RT-qPCR for the proinflammatory cytokines IL-1β, IL-6, IL-18, and TNF-α 2 hours after challenge, plotted as absolute values normalized by housekeeping gene expression (GAPDH). (E) ELISA for TNF-α in the RHEs supernatant at 2 and 24 hours after the challenge. n = 3 experiments, plotted as average ± SEM, analyzed by paired t-test (A–D) or two-way ANOVA followed by Tukey's post-hoc test (E); $^{*}p < 0.05$, $^{**}p < 0.01$, $^{****}p < 0.0001$). Abbreviations: GAPDH, Glyceraldehyde-3-phosphate dehydrogenase; RHE, reconstructed human epidermis.

cation ratio. We found that Oα-Syn-challenged HEKn (1.35 ± 0, $p < 0.0001$) had a higher nuclear/cytoplasm NF-kB fluorescence intensity, equivalent to TNF-α-challenged HEKn (1.28 ± 0.01, $p < 0.0001$) when compared with control (1.06 ± 0) (Fig. 3).

3.3. Oα-Syn increases expression and release of cytokines by RHE and its degenerative effect is partially blocked by cytokine inhibitors

As Oα-Syn induced NF-kB nuclear translocation, which is a transcription factor involved in the regulation of several inflammatory genes, we asked whether Oα-Syn could increase the expression of proinflammatory cytokines in the RHE. For this purpose, RHEs were then treated with 10 μM Oα-Syn for 2 hours. Subsequently, the mRNA expression of IL-1β, IL-6, IL-18, and TNF-α, was analyzed by RT-qPCR. We found that Oα-Syn caused an increase in IL-1β (Control: 0; Oα-Syn: 0.4, $p < 0.05$) and TNF-α (Control: 0; Oα-Syn: 0.18 ± 0.03, $p < 0.05$) mRNA levels compared with control (Fig. 4A and D). Other tested cytokines did not have their mRNA levels significantly changed (IL-18 control: 0.1 ± 0.03; Oα-Syn: 0.06 ± 0.02 and IL-6 control: 0.58 ± 7.35; Oα-Syn: 0) (Fig. 4B and C).

Of the two pro-inflammatory cytokines that had increased expression after treatment, TNF-α was of particular interest, since it had a similar effect to Oα-Syn in decreasing keratinocyte proliferation. To ensure that there was also more TNF-α being released after incubation with Oα-Syn, this cytokine was quantified in the supernatant by ELISA. Indeed, TNF-α release increased following Oα-Syn insult in a time-dependent manner (Oα-Syn 2h vs. Oα-Syn 24h, $p < 0.01$) compared with control (Control 2h: 0; Oα-Syn 2h: 864.3 ± 172.75 pg/mL, $p < 0.05$; Control 24h: 7.2 ± 3.74 pg/mL; Oα-Syn 24h: 2,215 ± 264.52 pg/mL, $p < 0.0001$) (Fig. 4E).

Since Oα-Syn decreased proliferation and increased TNF-α and IL-1β expression in keratinocytes, we investigated whether the proliferation-inhibiting effect of Oα-Syn on these cells was due to inflammation, namely through the release of these cytokines. To test this hypothesis, we treated keratinocytes with an IL-1β inhibitor (Kineret, 25 μg/mL), a TNF-α inhibitor (Etanercept, 500 μg/mL), or dexamethasone (Diprospan, 10 μM) along with 10 μM

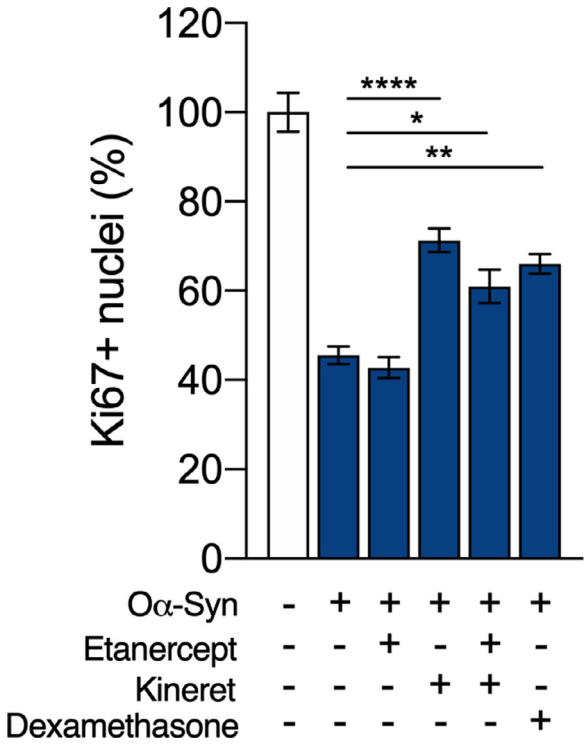

Fig. 5. Dexamethasone and IL-1β inhibitor partially prevent the anti-proliferative effect of Oα-Syn in HEKn. HEKn were treated or not with dexamethasone or tumor necrosis factor-alpha (TNF-α) (Etanercept, 500 µg/mL), or interleukin (IL)-1β (Kineret, 25 µg/mL) inhibitors along with Oligomeric α-Synuclein (Oα-Syn) for 24 hours. Percentage of Ki67 + cells relative to control (n = 2 experiments, plotted as average ± SEM, analyzed by one-way ANOVA followed by Tukey's post-hoc test; $^{*}p < 0.05$, $^{**}p < 0.01$, $^{****}p < 0.0001$). Abbreviation: HEKn, human neonatal epidermal keratinocytes.

Oα-Syn. Twenty four hours later the cells were fixed and immunostained for Ki67, and the percentage of proliferation relative to control was determined. We confirmed that Oα-Syn (45.56 ± 3.99%, $p < 0.0001$) decreased keratinocyte proliferation compared with control, and found that the IL-1β inhibitor (71.3 ± 4.74%, $p < 0.0001$) and dexamethasone (66.04 ± 4.74%, $p < 0.01$), but not the TNF-α inhibitor alone (42.75 ± 3.9%, $p < 0.05$), partially inhibited the anti-proliferative effect of Oα-Syn (Fig. 5).

4. Discussion

The aggregation of proteins and peptides, such as α-Syn, Aβ, and tau, is one of the hallmarks of age-related neuroinflammation (Glass et al., 2010). A growing body of evidence supports the presence of these aggregates also outside of the central nervous system. For instance, both monomeric and oligomeric α-Syn were described in the plasma, cerebrospinal fluid (Park et al., 2011), and basal tears from patients with Parkinson's disease but also from healthy elderly (Hamm-Alvarez et al., 2019). Phosphorylated-αSyn, which is a post-translational modification of α-Syn that promotes toxic aggregation, was found in postmortem skin biopsies from individuals with non-synucleinopathic neurodegenerative diseases and from one non-neurodegenerative control (Wang et al., 2021). In addition, α-Syn expression was observed in the skin of patients with α-synucleinopathies as well as healthy individuals (Rodriguez-Leyva et al., 2017). Oα-Syn and phosphorylated-αSyn were found within autonomic skin nerve fibers from individuals with Parkinson's disease and other αSynucleinopathies, respectively (Donadio et al., 2018; Mazzetti et al., 2020), with differences in localization and loading according to the specific synucleinopathy (Donadio et al., 2018). Using spectroscopy of human skin biopsy samples, Akerman and collaborators (2019) showed that some amyloidogenic proteins, including α-Syn, build up as the skin ages. Even though it is not necessarily an aging model, we also found α-Syn expression in the RHE.

The expression of α-Syn in the skin has been mainly ascribed to peripheral nerve terminals and melanocytes (Kim et al., 2019; Rodriguez-Leyva et al., 2017). Dermal fibroblasts are also another possible source of α-Syn accumulation in the aged skin, releasing exosomes containing α-Syn and pro-inflammatory mediators by cell-to-cell transmission from the dermis to the epidermis (Cerri et al., 2021; Danzer et al., 2012). Furthermore, a study showed α-Syn immunopositive keratinocytes from the skin of patients with Parkinson's disease and atypical parkinsonism (Rodríguez-Leyva et al., 2014). Additionally, Akerman et al. (2019) detected α-Syn throughout the epidermal layer from human skin samples. Interestingly, misfolded α-Syn can propagate from the gut to the brain but also to several peripheral organs and tissues, including the skin (Van Den Berge et al., 2021). Regardless of the source, both monomeric and oligomeric α-Syn species might coexist in the epidermis, as seen in other tissues, and aggregation of monomeric α-Syn might occur at some level as the skin ages.

Interestingly, exogenous Oα-Syn decreased epidermal thickness, which is similar to what happens in senior skin as a result of a decrease in cellular proliferation and reduced innervation (Besné et al., 2002; Gilhar et al., 2004). In this work, we found that both exogenous TNF-α and, more pronouncedly, Oα-Syn, decreased cellular proliferation. TNF-α represses the transcription of genes implicated in the cell cycle in human keratinocytes (Banno et al., 2004; Kono et al., 1990; Pillai et al., 1989), and inhibits human keratinocyte proliferation in vitro (Detmar and Orfanos, 1990). With regard to Oα-Syn, this is the first evidence that this aggregate hampers keratinocyte proliferation. However, It has been shown that forced expression of α-Syn causes deregulation of genes involved in the cell cycle, including downregulation of Ki67, in Lund human mesencephalic and H4 neuroglioma cells (Pinho et al., 2019). Verma et al. (2021) demonstrated that the protein levels of p21, a cell cycle-arrester and senescence marker, were higher in human Parkinson's disease postmortem substantia nigra pars compacta than in control samples.

One way Oα-Syn might be toxic to keratinocytes is triggering inflammation, and it is well-known that this aggregate plays a notable role in neuroinflammation. NF-kB is considered the central regulator of inflammatory processes and, not coincidentally, the transcription factor most associated with aging (Tilstra et al., 2011). Both TNF-α and UVB-irradiation induce NF-kB DNA-binding activity in human keratinocytes (Lewis and Spandau, 2007). Here we demonstrated for the first time that Oα-Syn also elicited NF-kB nuclear translocation in keratinocytes. One of the mechanisms by which extracellular Oα-Syn exerts its toxic effects on microglia and astrocytes is through activating Toll-like receptors 1, 2, or 4. This activation, in turn, leads to the nuclear translocation of NF-kB, which triggers the expression of proinflammatory cytokines, such as IL-6, TNF-α, and IL-1β. Human keratinocytes express Toll-like receptors 1, 2, and 4 (Köllisch et al., 2005; Pivarcsi et al., 2004). Therefore, Toll-like receptors might play a role in the Oα-Syn-mediated toxic effects observed in keratinocytes.

Herein, we showed that besides causing nuclear translocation of NF-kB, exogenous Oα-Syn caused overexpression of the proinflammatory cytokines IL-1β and TNF-α. Indeed, studies have been shown that Oα-Syn causes the release of several pro-inflammatory

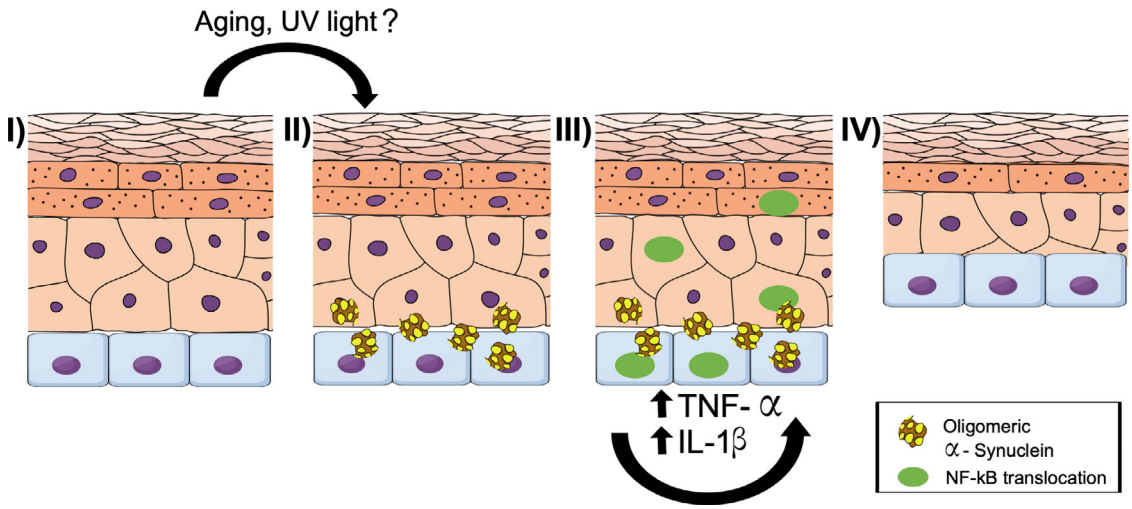

Fig. 6. The working hypothesis for the role of oligomeric α-Synuclein in skin degeneration with aging. (I) Ultraviolet (UV) exposure and aging might contribute to oligomerization of available α-Synuclein. (II) α-Synuclein aggregates and accumulates in the epidermis. (III) oligomeric α-Synuclein activates inflammatory responses in keratinocytes, via Nuclear factor-κB (NF-kB) translocation to the nucleus (represented by green nuclei) and triggers the transcription and autocrine release of inflammatory cytokines, such as tumor necrosis factor-alpha (TNF-α) and interleukin (IL)-1β. (IV) One of the observed effects of these cytokines on the epidermis is the reduced keratinocyte proliferation, which contributes to skin degeneration and, ultimately, to epidermal thinning, characteristic of aged skin. Illustration prepared with Mind the Graph (https://mindthegraph.com). (For interpretation of the references to color in this figure legend, the reader is referred to the Web version of this article.)

cytokines (Roodveldt et al., 2010). In line with this work, Oα-Syn increased TNF-α expression and release from RHE. However, exogenously but not endogenously-induced TNF-α decreased proliferation in the RHE. One hypothesis is that the endogenous levels of TNF-α released following Oα-Syn administration were not sufficient to cause a direct antiproliferative effect in the RHE, as seen when exogenous 20 ng/mL TNF-α was administered. On the other hand, Oα-Syn-induced endogenous IL-1β had an antiproliferative effect in the RHE, which was partially blocked by its cytokine inhibitor. IL-1β is released by activation of the NLR family pyrin domain containing 3 inflammasome, which has also been implicated in Oα-Syn-induced responses by microglia (Trudler et al., 2021). Additionally, both cytokines, IL-1β and TNF-α, when overexpressed, may trigger positive feedback of themselves and of other proinflammatory cytokines previously described in skin inflammaging studies (Fuller, 2019; Pilkington et al., 2021; Zhuang and Lyga, 2014). This can result in keratinocyte loss, epidermal degeneration, and ultimately, fine lines and impaired mechanical skin properties.

α-Syn is poorly expressed in the RHE and, as a prion-like protein, it can be transported by cell-to-cell propagation. Accordingly, our hypothesis is that peripheral nerve terminals and melanocytes convey α-Syn to the epidermis. Interestingly, α-Syn is found in postmortem tissues of the peripheral nervous system from patients with α-synucleinopathy (Sumikura et al., 2015), in sensory nerve terminals in the skin (Akerman et al., 2019), and in sensory neurons derived from human induced pluripotent stem cells (Guimarães et al., 2018). Therefore, simply by accumulation or via other factors, such as UV radiation (Carmo-Gonçalves et al., 2014), α-Syn could aggregate into Oα-Syn, causing epidermal inflammation and degeneration (Fig. 6).

It is noteworthy that epidermal degeneration was partially caused by Oα-Syn-related inflammation, therefore Oα-Syn may also act by other mechanisms. Indeed, Oα-Syn-induced toxicity is complex and has not been completely unveiled. For instance, studies have shown that this aggregate can be incorporated into neurons and damage organelles, such as mitochondria (Park et al., 2020) and lysosomes (Senol et al., 2021), hampering cellular metabolism.

5. Conclusions

Oα-Syn remarkably affected the epidermal basal layer, which is critical to tissue regeneration because it mostly contains proliferative keratinocytes. Decreased proliferation caused by Oα-Syn yielded a thin epidermis as seen in sun-damaged, aged, as well as diseased skin. Our translational cellular models allow the understanding of aspects of skin aging, observed in clinical studies related to neurodegenerative diseases, but also important on skin homeostasis in aging. This study opens new avenues for therapies targeting Oα-Syn accumulation in the skin, important not only for skin degeneration caused by neurodegenerative diseases but also by normal aging. Further studies focusing on Oα-Syn incorporation and organelles damaging might clarify additional mechanisms by which Oα-Syn promotes skin degeneration.

Credit author statement

Julia Oliveira: Conceptualization, Formal analysis, Investigation, Writing - Original Draft. **Vanja Dakic:** Conceptualization, Investigation, Writing - Original Draft. **Gabriela Vitória:** Conceptualization, Investigation, Writing - Review & Editing. **Carolina Pedrosa:** Conceptualization, Investigation, Writing - Review & Editing. **Mayara Mendes:** Investigation, Writing - Review & Editing. **Luiz Guilherme Aragão:** Conceptualization, Investigation, Writing - Review & Editing. **Thyago Cardim-Pires:** Investigation. **Damien Lelièvre:** Investigation. **Daniel Rodrigues Furtado:** Conceptualization. **Roberta O. Pinheiro:** Resources. **Débora Foguel:** Resources, Writing - Review & Editing. **Lionel Breton:** Supervision. **Charbel Bouez:** Supervision. **Rodrigo De Vecchi:** Conceptualization, Resources, Writing - Original Draft. **Marília Guimarães:** Conceptualization, Supervision, Writing - Original Draft, Project administration. **Stevens Rehen:** Writing - Review & Editing, Supervision, Project administration, Funding acquisition.

Disclosure statement

VD and RDV are employees of L'Oréal Research & Innovation. The authors declare that there are no conflicts of interest.

Acknowledgements

This work was supported by L'Oréal Research & Innovation.

The authors thank Coordenação de Aperfeiçoamento de Pessoal de Nível Superior (CAPES) for the scholarship to Carolina Pedrosa and Luiz Guilherme Aragão. The authors also thank Dr Emiliano Medei for the kind gift of Kineret and for helpful comments.

Supplementary materials

Supplementary material associated with this article can be found, in the online version, at doi:10.1016/j.neurobiolaging.2022.02.010.

References

Akerman, S.C., Hossain, S., Shobo, A., Zhong, Y., Jourdain, R., Hancock, M.A., George, K., Breton, L., Multhaup, G., 2019. Neurodegenerative disease-related proteins within the epidermal layer of the human skin. J. Alzheimers Dis. 69, 463–478. doi:10.3233/JAD-181191.

Alvarez-Erviti, L., Couch, Y., Richardson, J., Cooper, J.M., Wood, M.J., 2011. Alpha-synuclein release by neurons activates the inflammatory response in a microglial cell line. Neurosci. Res. 69, 337–342.

Banno, T., Gazel, A., Blumenberg, M., 2004. Effects of tumor necrosis factor-alpha (TNF alpha) in epidermal keratinocytes revealed using global transcriptional profiling. J. Biol. Chem. 279, 32633–32642. doi:10.1074/jbc.M400642200.

Baumann, L., 2007. Skin ageing and its treatment. J. Pathol. 211, 241–251. doi:10.1002/path.2098.

Beach, T.G., Adler, C.H., Sue, L.I., Vedders, L., Lue, L., White III, C.L., Akiyama, H., Caviness, J.N., Shill, H.A., Sabbagh, M.N., 2010. Multi-organ distribution of phosphorylated α-synuclein histopathology in subjects with Lewy body disorders. Acta Neuropathol. 119, 689–702.

Besné, I., Descombes, C., Breton, L., 2002. Effect of age and anatomical site on density of sensory innervation in human epidermis. Arch Dermatol 138, 1445–1450. doi:10.1001/archderm.138.11.1445.

Braak, H., Del Tredici, K., 2017. Neuropathological staging of brain pathology in sporadic Parkinson's disease: separating the wheat from the chaff. J. Parkinson's Dis. 7, S71–S85.

Braga, C.A., Follmer, C., Palhano, F.L., Khattar, E., Freitas, M.S., Romão, L., Di Giovanni, S., Lashuel, H.A., Silva, J.L., Foguel, D., 2011. The anti-Parkinsonian drug selegiline delays the nucleation phase of α-synuclein aggregation leading to the formation of nontoxic species. J Mol Biol 405 (1), 254–273. doi:10.1016/j.jmb.2010.10.027.

Carmo-Gonçalves, P., Pinheiro, A.S., Romao, L., Cortines, J., Follmer, C., 2014. UV-induced selective oxidation of Met5 to Met-sulfoxide leads to the formation of neurotoxic fibril-incompetent α-synuclein oligomers. Amyloid 21, 163–174.

Cerri, S., Ghezzi, C., Ongari, G., Croce, S., Avenali, M., Zangaglia, R., Di Monte, D.A., Valente, E.M., Blandini, F., 2021. GBA mutations influence the release and pathological effects of small extracellular vesicles from fibroblasts of patients with Parkinson's Disease. Int. J. Mol. Sci. 22, 2215.

Danzer, K.M., Kranich, L.R., Ruf, W.P., Cagsal-Getkin, O., Winslow, A.R., Zhu, L., Vanderburg, C.R., McLean, P.J., 2012. Exosomal cell-to-cell transmission of alpha synuclein oligomers. Mol. Neurodegener. 7, 1–18.

Detmar, M., Orfanos, C.E., 1990. Tumor necrosis factor-alpha inhibits cell proliferation and induces class II antigens and cell adhesion molecules in cultured normal human keratinocytes in vitro. Arch Dermatol Res 282, 238–245. doi:10.1007/BF00371643.

Donadio, V., Incensi, A., El-Agnaf, O., Rizzo, G., Vaikath, N., Del Sorbo, F., Scaglione, C., Capellari, S., Elia, A., Maserati, M.S., Pantieri, R., Liguori, R., 2018. Skin α-synuclein deposits differ in clinical variants of synucleinopathy: an in vivo study. Sci. Rep. 8 (1), 14246. doi:10.1038/s41598-018-32588-8.

Fernandes, L., Messias, B., Pereira-Neves, A., Azevedo, E.P., Araújo, J., Foguel, D., Palhano, F.L., 2020. Green tea polyphenol microparticles based on the oxidative coupling of EGCG Inhibit amyloid aggregation/cytotoxicity and serve as a platform for drug delivery. ACS Biomater Sci Eng 6 (8), 4414–4423. doi:10.1021/acsbiomaterials.0c00188.

Fuller, B., 2019. Role of PGE-2 and other inflammatory mediators in skin aging and their inhibition by topical natural anti-inflammatories. Cosmetics 6, 6.

Gelpi, E., Navarro-Otano, J., Tolosa, E., Gaig, C., Compta, Y., Rey, M.J., Martí, M.J., Hernández, I., Valldeoriola, F., Reñé, R., 2014. Multiple organ involvement by alpha-synuclein pathology in Lewy body disorders. Mov. Disord. 29, 1010–1018.

Gilhar, A., Ullmann, Y., Karry, R., Shalaginov, R., Assy, B., Serafimovich, S., Kalish, R.S., 2004. Ageing of human epidermis: the role of apoptosis, Fas and telomerase. Br. J. Dermatol. 150, 56–63. doi:10.1111/j.1365-2133.2004.05715.x.

Glass, C.K., Saijo, K., Winner, B., Marchetto, M.C., Gage, F.H., 2010. Mechanisms underlying inflammation in neurodegeneration. Cell 140, 918–934. doi:10.1016/j.cell.2010.02.016.

Grinberg-Bleyer, Y., Dainichi, T., Oh, H., Heise, N., Klein, U., Schmid, R.M., Hayden, M.S., Ghosh, S., 2015. Cutting edge: NF-κB p65 and c-Rel control epidermal development and immune homeostasis in the skin. J. Immunol. 194, 2472–2476.

Guimarães, M.Z.P., De Vecchi, R., Vitória, G., Sochacki, J.K., Paulsen, B.S., Lima, I., Rodrigues da Silva, F., da Costa, R.F.M., Castro, N.G., Breton, L., Rehen, S.K., 2018. Generation of iPSC-Derived human peripheral sensory neurons releasing substance P elicited by TRPV1 agonists. Front Mol Neurosci 11, 277. doi:10.3389/fnmol.2018.00277.

Hamm-Alvarez, S.F., Okamoto, C.T., Janga, S.R., Feigenbaum, D., Edman, M.C., Freire, D., Shah, M., Ghanshani, R., Mack, W.J., Lew, M.F., 2019. Oligomeric α-synuclein is increased in basal tears of Parkinson's patients. Biomark. Med. 13, 941–952.

Heinonen, O., Soininen, H., Syrjänen, S., Neittaanmäki, H., Paljärvi, L., Kosunen, O., Syrjänen, K., Riekkinen, P., 1994. beta-Amyloid protein immunoreactivity in skin is not a reliable marker of Alzheimer's disease. An autopsy-controlled study. Arch. Neurol. 51, 799–804. doi:10.1001/archneur.1994.00540200075019.

Joyce, D., Albanese, C., Steer, J., Fu, M., Bouzahzah, B., Pestell, R.G., 2001. NF-kappaB and cell-cycle regulation: the cyclin connection. Cytokine Growth Factor Rev 12, 73–90. doi:10.1016/s1359-6101(00)00018-6.

Lashuel, H.A., Overk, C.R., Oueslati, A., Masliah, E., 2013. The many faces of α-synuclein: from structure and toxicity to therapeutic target. Nat Rev Neurosci 14 (1), 38–48. doi:10.1038/nrn3406.

Kim, J.Y., Illigens, B.M., McCormick, M.P., Wang, N., Gibbons, C.H., 2019. Alpha-synuclein in skin nerve fibers as a biomarker for alpha-synucleinopathies. J. Clin. Neurol. (Seoul, Korea) 15, 135–142.

Köllisch, G., Kalali, B.N., Voelcker, V., Wallich, R., Behrendt, H., Ring, J., Bauer, S., Jakob, T., Mempel, M., Ollert, M., 2005. Various members of the Toll-like receptor family contribute to the innate immune response of human epidermal keratinocytes. Immunology 114, 531–541.

Kono, T., Tanii, T., Furukawa, M., Mizuno, N., Taniguchi, S., Ishii, M., Hamada, T., 1990. Effects of human recombinant Tumor Necrosis Factor-α (TNF-α) on the proliferative potential of human keratinocytes cultured in serum-free medium. J. Dermatol. 17, 409–413.

Krüger, R., Kuhn, W., Müller, T., Woitalla, D., Graeber, M., Kösel, S., Przuntek, H., Epplen, J.T., Schöls, L., Riess, O., 1998. Ala30Pro mutation in the gene encoding alpha-synuclein in Parkinson's disease. Nat. Genet. 18, 106–108. doi:10.1038/ng0298-106.

Kumar, S.T., Donzelli, S., Chiki, A., Syed, M.M.K., Lashuel, H.A., 2020. A simple, versatile and robust centrifugation-based filtration protocol for the isolation and quantification of α-synuclein monomers, oligomers and fibrils: towards improving experimental reproducibility in α-synuclein research. J Neurochem 153 (1), 103–119. doi:10.1111/jnc.14955.

Lan, C.-C.E., Yu, H.-S., Wu, C.-S., Kuo, H.-Y., Chai, C.-Y., Chen, G.-S., 2005. FK506 inhibits tumour necrosis factor-alpha secretion in human keratinocytes via regulation of nuclear factor-kappaB. Br. J. Dermatol. 153, 725–732. doi:10.1111/j.1365-2133.2005.06779.x.

Lewis, D.A., Spandau, D.F., 2007. UVB activation of NF-κB in normal human keratinocytes occurs via a unique mechanism. Arch. Dermatol. Res. 299, 93–101.

Martires, K.J., Fu, P., Polster, A.M., Cooper, K.D., Baron, E.D., 2009. Factors that affect skin aging: a cohort-based survey on twins. Arch Dermatol 145, 1375–1379. doi:10.1001/archdermatol.2009.303.

Mazzetti, S., Basellini, M.J., Ferri, V., Cassani, E., Cereda, E., Paolini, M., Calogero, A.M., Bolliri, C., De Leonardis, M., Sacilotto, G., Cilia, R., Cappelletti, G., Pezzoli, G., 2020. α-Synuclein oligomers in skin biopsy of idiopathic and monozygotic twin patients with Parkinson's disease. Brain 143, 920–931. doi:10.1093/brain/awaa008.

Montoliu-Gaya, L., Mulder, S.D., Veerhuis, R., Villegas, S., 2017. Effects of an Aβ-antibody fragment on Aβ aggregation and astrocytic uptake are modulated by apolipoprotein E and J mimetic peptides. PLoS One 12 (11), e0188191. doi:10.1371/journal.pone.0188191.

Park, J., Burgess, J.D., Faroqi, A.H., DeMeo, N.N., Fiesel, F.C., Springer, W., Delenclos, M., McLean, P.J., 2020. Alpha-synuclein-induced mitochondrial dysfunction is mediated via a sirtuin 3-dependent pathway. Mol. Neurodegener. 15 (1), 5. doi:10.1186/s13024-019-0349-x.

Park, M.J., Cheon, S.-M., Bae, H.-R., Kim, S.-H., Kim, J.W., 2011. Elevated levels of α-synuclein oligomer in the cerebrospinal fluid of drug-naïve patients with Parkinson's disease. J. Clin. Neurol. (Seoul, Korea) 7, 215–222.

Pilkington, S.M., Bulfone-Paus, S., Griffiths, C.E., Watson, R.E., 2021. Inflammaging and the Skin. J. Invest. Dermatol 141 (4S), 1087–1095. doi:10.1016/j.jid.2020.11.006.

Pillai, S., Bikle, D.D., Eessalu, T.E., Aggarwal, B.B., Elias, P.M., 1989. Binding and biological effects of tumor necrosis factor alpha on cultured human neonatal foreskin keratinocytes. J. Clin. Invest. 83, 816–821.

Pinho, R., Paiva, I., Jercic, K.G., Fonseca-Ornelas, L., Gerhardt, E., Fahlbusch, C., Garcia-Esparcia, P., Kerimoglu, C., Pavlou, M.A.S., Villar-Piqué, A., Szego, É., Fonseca, T.L., Odoardi, F., Soeroes, S., Rego, A.C., Fischle, W., Schwamborn, J.C., Meyer, T., Kügler, S., Ferrer, I., Attems, J., Fischer, A., Becker, S., Zweckstetter, M., Borovecki, F., Outeiro, T.F., 2019. Nuclear localization and phosphorylation modulate pathological effects of alpha-synuclein. Hum. Mol. Genet. 28 (1), 31–50. doi:10.1093/hmg/ddy326.

Pivarcsi, A., Kemény, L., Dobozy, A., 2004. Innate immune functions of the keratinocytes. Acta Microbiol. Immunol. Hung. 51, 303–310.

Pupe, A., Degreef, H., Garmyn, M., 2003. Induction of tumor necrosis factor-alpha by UVB: a role for reactive oxygen intermediates and eicosanoids. Photochem. Photobiol. 78, 68–74. doi:10.1562/0031-8655(2003)078<0043:mmitmc>2.0.co;2.

Rodríguez-Leyva, I., Calderón-Garcidueñas, A.L., Jiménez-Capdeville, M.E., Rentería–Palomo, A.A., Hernandez-Rodriguez, H.G., Valdés-Rodríguez, R., Fuentes-Ahumada, C., Torres-Álvarez, B., Sepúlveda-Saavedra, J., Soto-Domínguez, A., 2014. α-Synuclein inclusions in the skin of Parkinson's disease and parkinsonism. Ann. Clin. Transl. Neurol. 1, 471–478.

Rodriguez-Leyva, I., Chi-Ahumada, E., Mejía, M., Castanedo-Cazares, J.P., Eng, W., Saikaly, S.K., Carrizales, J., Levine, T.D., Norman, R.A., Jimenez-Capdeville, M.E., 2017. The presence of alpha-Synuclein in skin from melanoma and patients with Parkinson's disease. Mov. Disord. Clin. Pract. 4, 724–732. doi:10.1002/mdc3.12494.

Roodveldt, C., Labrador-Garrido, A., Gonzalez-Rey, E., Fernandez-Montesinos, R., Caro, M., Lachaud, C.C., Waudby, C.A., Delgado, M., Dobson, C.M., Pozo, D., 2010. Glial innate immunity generated by non-aggregated alpha-synuclein in mouse: differences between wild-type and Parkinson's disease-linked mutants. PLoS One 5, e13481.

Rosdy, M., Clauss, L.C., 1990. Terminal epidermal differentiation of human keratinocytes grown in chemically defined medium on inert filter substrates at the air-liquid interface. J. Invest. Dermatol. 95, 409–414. doi:10.1111/1523-1747.ep12555510.

Senol, A.D., Samarani, M., Syan, S., Guardia, C.M., Nonaka, T., Liv, N., Latour-Lambert, P., Hasegawa, M., Klumperman, J., Bonifacino, J.B., Zurzolo, C., 2021. α-Synuclein fibrils subvert lysosome structure and function for the propagation of protein misfolding between cells through tunneling nanotubes. PLoS Biol. 19 (7), e3001287. doi:10.1371/journal.pbio.3001287.

Sumikura, H., Takao, M., Hatsuta, H., Ito, S., Nakano, Y., Uchino, A., Nogami, A., Saito, Y., Mochizuki, H., Murayama, S., 2015. Distribution of α-synuclein in the spinal cord and dorsal root ganglia in an autopsy cohort of elderly persons. Acta Neurophatol Commun 3. doi:10.1186/s40478-015-0236-9.

Tilstra, J.S., Clauson, C.L., Niedernhofer, L.J., Robbins, P.D., 2011. NF-κB in aging and disease. Aging Dis 2, 449–465.

Tornier, C., Roquet, M., de Fraissinette, A.de B., 2010. Adaptation of the validated SkinEthic™ Reconstructed Human Epidermis (RHE) skin corrosion test method to 0.5 cm2 tissue sample. Toxicol. in Vitro 24, 1379–1385.

Trudler, D., Nazor, K.L., Eisele, Y.S., Grabauskas, T., Dolatabadi, N., Parker, J., Sultan, A., Zhong, Z., Goodwin, M.S., Levites, Y., 2021. Soluble α-synuclein–antibody complexes activate the NLRP3 inflammasome in hiPSC-derived microglia. Proc. Natl. Acad. Sci. 118.

Van Den Berge, N., Ferreira, N., Mikkelsen, T.W., Alstrup, A.K.O., Tamgüney, G., Karlsson, P., Terkelsen, A.J., Nyengaard, J.R., Jensen, P.H., Borghammer, P., 2021. Animal models of brain-first and body-first Parkinson's disease. Brain 144, 1853–1868. doi:10.1093/brain/awab061.

Vecchi, R.D., Dakic, V., Mattos, G., Rigaudeau, A.-S., Oliveira, V., Garcia, C., Alépée, N., Cotovio, J., Bouez, C., 2018. Implementation, availability and regulatory status of an OECD accepted Reconstructed Human Epidermis model in Brazil. Vigilância Sanitária em Debate: Sociedade, Ciência & Tecnologia 6, 64–71. doi:10.22239/2317-269x.01055.

Verma, D.K., Seo, B.O., Ghosh, A., Ma, S., Hernandez-Quijada, K., Andersen, J.K., Ko, H.S., Kim, Y., 2021. Alpha-Synuclein preformed fibrils induce cellular senescence in Parkinson's disease models. Cells 10 (7), 1694 10.3390/cells10071694.

Wakabayashi, K., Takahashi, H., Ohama, E., Ikuta, F., 1990. Parkinson's disease: an immunohistochemical study of Lewy body-containing neurons in the enteric nervous system. Acta Neuropathol. 79, 581–583.

Wang, Y., Wang, L., Wen, X., Hao, D., Zhang, N., He, G., Jiang, X., 2019. NF-κB signaling in skin aging. Mech. Ageing Dev. 184, 111160.

Wang, Z., Becker, K., Donadio, V., Siedlak, S., Yuan, J., Rezaee, M., Incensi, A., Kuzkina, A., Orrú, C.D., Tatsuoka, C., 2021. Skin α-synuclein aggregation seeding activity as a novel biomarker for Parkinson disease. JAMA Neurol. 78, 30–40.

Zhuang, Y., Lyga, J., 2014. Inflammaging in skin and other tissues-the roles of complement system and macrophage. Inflammation & Allergy-Drug Targets (Formerly Current Drug Targets-Inflammation & Allergy)(Discontinued) 13, 153–161.